World Journal of Advanced Research and Reviews
eISSN: 2581-9615 CODEN (USA): WJARAI
Cross Ref DOI: 10.30574/wjarr
Journal homepage: https://wjarr.com/

(RESEARCH ARTICLE)

Check for updates

Optimizing LSM-LSF composite cathodes for enhanced solid oxide fuel cell performance: Material engineering and electrochemical insights

Ramin Babazadeh Dizaj [1,*] and Nastaran Sabahi [2]

[1] *Center for Energy Storage Materials and Devices, Department of Metallurgical and Materials Engineering, Middle East Technical University, Ankara, Turkey.*
[2] *Department of Civil Engineering, Middle East Technical University, Ankara, Turkey.*

World Journal of Advanced Research and Reviews, 2023, 20(01), 1284–1291

Publication history: Received on 16 September 2023; revised on 26 October 2023; accepted on 28 October 2023

Article DOI: https://doi.org/10.30574/wjarr.2023.20.1.2183

Abstract

In response to pressing environmental concerns and the ever-increasing global energy demand, the pursuit of sustainable energy sources has garnered substantial momentum. A predominant focus of research within this domain revolves around the enhancement of solid oxide fuel cell performance, with particular attention directed toward the intricate oxygen reduction reaction transpiring at the cathode electrode. The present investigation embarks upon the exploration of a composite material comprising $La_{1-x}Sr_xMnO_{3-\delta}$ (LSM) and $La_{1-x}Sr_xFeO_{3-\delta}$ (LSF) as prospective cathode materials. However, the achievement of optimal composite cathodes necessitates the application of advanced materials engineering strategies. The principal aim of this comprehensive study is the development of high-performance composite cathodes, achieved through the deposition of thin film counterparts onto scandium-stabilized zirconia (ScSZ) electrolyte substrate employing the precision sputtering technique. The ensuing findings unequivocally unveil the remarkable performance exhibited by this innovative composite cathode configuration, notably manifesting its excellence at an operating temperature as modest as 780 °C. These promising outcomes imbue optimism regarding the prospective utilization of this composite material in advanced energy conversion applications, marking a significant advancement toward the realization of sustainable and efficient energy systems.

Keywords: Solid oxide fuel cell; Cathode electrode; LSM-LSF; Area-specific resistance; Oxygen reduction reaction; Sputtering

1. Introduction

The pursuit of sustainable and diverse energy sources has gained momentum due to the substantial environmental impacts resulting from conventional energy resources and the escalating global energy demand [1-9]. One particular area of focus in this endeavor revolves around enhancing the performance of energy conversion devices, notably solid oxide fuel cells (SOFCs) [10, 11] and batteries [12, 13]. SOFCs, in particular, stand out as a highly promising category of sustainable energy technologies designed to convert the chemical energy stored in hydrogen-containing fuels into electrical energy [14, 15]. Nevertheless, the efficiency of SOFCs faces a significant challenge primarily attributed to the sluggish oxygen reduction reaction (ORR) occurring at the cathode electrode [16]. In order to attain superior ORR activity, the cathode material must possess exceptional catalytic capabilities for both oxygen adsorption and dissociation, in addition to demonstrating proficient electrical and ionic conductivity [17]. Furthermore, it is imperative that the chosen cathode material maintains chemical and thermal compatibility with the electrolyte while simultaneously facilitating the permeability of gases [18].

* Corresponding author: Ramin Babazadeh Dizaj.

Oxide materials, specifically, mixed ionic and electronic structures (MIECs) have emerged as a focal area of investigation in the realm of energy materials [19-24] Notably, (La, Sr)$MnO_{3-\delta}$ (LSM) [25, 26] and (La, Sr)$FeO_{3-\delta}$ (LSF) [27, 28] have exhibited considerable promise in enhancing the ORR performance. LSM possesses several advantageous characteristics as a cathode material, including high electrical conductivity, compatibility with zirconia-based electrolytes, and sufficient catalytic activity. However, its utilization as a sole cathode material is hampered by its relatively low ionic conductivity at intermediate working temperatures, resulting in suboptimal electrochemical performance [29, 30]. To address this challenge, researchers have explored the incorporation of high oxygen ion conductors, such as electrolyte materials, into LSM-based cathodes. A notable example is the work of Jeong et al. [31], who studied LSM-ScSZ composite cathodes with varying compositions. Among these, LSM60ScSZ40 exhibited the most favorable characteristics, boasting the lowest total impedance value of 0.031 Ω cm^2 at 900 °C. On the other hand, LSF exhibits commendable electronic and ionic conductivity, along with high catalytic activity, particularly at low oxygen partial pressures. However, it displays diminished stability under high oxygen partial pressures [32]. Interestingly, Tang et al. [33] explored the feasibility of utilizing mixed compositions of LSM and LSF as cathode materials in full cell measurements. Their findings unveiled that the cell performance of the LSM-LSF solid solution significantly outperformed those utilizing LSM or LSF cathodes independently. This outcome underscores the considerable advantages associated with employing the LSM-LSF mixture as a cathode material, shedding light on the potential for enhancing the efficiency and performance of SOFCs for sustainable energy conversion applications.

Nevertheless, achieving the desired characteristics of LSM-LSF composites necessitates concerted efforts in materials engineering. These endeavors can be channeled towards the incorporation of oxide nanostructures and the fabrication of thin films using advanced physical vapor deposition techniques like sputtering or pulsed laser deposition (PLD) [34-37]. A primary concern when developing thin film materials for SOFCs is ensuring the structural, chemical, and thermal compatibility between the cathode and electrolyte components [37, 38]. In this context, scandium-stabilized zirconia (ScSZ), possessing a fluorite structure, stands out due to its exceptional ionic conductivity, particularly within the intermediate operating temperature range when compared to other ZrO_2-based electrolytes [39]. Moreover, ScSZ demonstrates favorable chemical compatibility with both LSM and LSF, with no evidence of solid solution formation even after prolonged testing [40, 41]. Its thermal expansion coefficient (TEC) of 11.9×10^{-6} $°C^{-1}$ [42] aligns closely with those of LSM (11.5×10-6/°C) [43] and LSF (12.6×10-6/°C) [44], further enhancing its suitability as an electrolyte material. Taken together, considering all the stringent compatibility requirements, ScSZ emerges as a highly suitable candidate for deployment as an electrolyte in conjunction with LSM-LSF composite cathodes for advanced SOFC applications.

The overarching objective of the current investigation is the development of optimized LSM-LSF composite cathodes tailored to enhance electrochemical performance in SOFCs. To achieve this objective, a systematic approach was employed, involving the deposition of thin LSM-LSF composite films as cathode materials onto ScSZ electrolyte substrates. The deposition process utilized a combinatorial geometry and was executed through the precise sputtering technique. Subsequently, the performance evaluation of these innovative cathodes was conducted using symmetrical cells as the testing platform, employing electrochemical impedance spectroscopy (EIS) as the primary analytical method. This systematic and methodical investigation aims to shed light on the electrochemical behavior of LSM-LSF composite cathodes and offer insights into their potential as high-performance components in solid oxide fuel cell technology.

2. Materials and Methods

ScSZ electrolyte substrates were fabricated through the tape casting method. The preparation of the slurry for tape casting occurred in two sequential steps. Firstly, 4.24 gr of ScSZ (Fuel Cell Material, USA) was mixed with 2.6 ml of Methyl ethyl ketone (MEK) as a solvent, 2.6 ml of ethanol as a solvent, and 0.17 gr of Triethanolamine as a dispersant. This mixture underwent ball milling for a duration of 2 hours. Subsequently, in the second step, 0.44 gr of polyvinyl butyral (PVB) was added as a binder, and 0.44 grams of polyethylene glycol (PEG) was introduced as a plasticizer. Ball milling was continued for an additional 2 hours. The resulting slurry was cast onto a mylar film with a blade gap set at 350 μm, and the slurry was cast at a speed of 7 mm per second. The mylar film utilized had a silicone coating to facilitate easy removal of the cast material. Following the casting process, the slip was allowed to air-dry for a duration of 2 hours. Subsequently, 20 mm diameter discs were punched out from the cast film. These electrolyte discs underwent sintering at elevated temperatures, leading to the formation of dense circular ScSZ electrolytes measuring 18 mm in diameter and 100 μm in thickness.

A magnetron sputtering vacuum deposition system, featuring a cubic chamber with dimensions of 500 × 500 × 500 mm^3, was employed for the deposition of composite LSM-LSF thin film cathodes (see Figure 1a). In this setup, six ScSZ substrates were simultaneously positioned within the substrate holder, which was situated 110 mm above the center

of the sputter targets. The experiments were conducted using two sputter guns, each equipped with 2-inch diameter LSM and LSF sputter targets placed at a tilted position, with a center-to-center distance of 125 mm. To ensure uniform film thickness across the sample holder, power loading was adjusted to 110 watts for LSM and 11 watts for LSF. Sputtering was carried out for a duration of 16 hours under a vacuum of 5 mTorr, with fixed Argon and Oxygen flow rates of 20 and 5 sccm, respectively. The resulting films from the co-sputtering process using LSM and LSF targets exhibited a diameter of 12 mm and a thickness of 500 nm. Subsequently, the discs were inverted, and composite cathodes were also deposited on the reverse side of the ScSZ substrates. To complete the setup, a circular gold coating, measuring 10 mm in diameter and 150 nm in thickness, was applied to the cathode surface as a current collector. A schematic representation of the fabricated symmetrical cells is depicted in Figures 1b and 1c.

To establish the sintering conditions, we employed Thermogravimetric Analysis (TGA), subjecting the samples to temperatures up to 800 °C. For microstructural examination of the thin composite films, scanning electron microscopy (SEM) was utilized, employing an FEI Nova Nano-SEM 430 instrument. The elemental composition of the composite films was assessed using an energy-dispersive X-ray spectroscopy (EDS) detector. Electrochemical assessments were conducted on symmetric cells, with electrochemical impedance spectroscopy (EIS) spectra recorded using a Gamry reference 3000 Potentiostat/Galvanostat. Attachment of gold wires to the gold-coated samples was facilitated using silver paste. The EIS spectra were collected with a 10-mV perturbation voltage, spanning a frequency range from 0.1 Hz to 0.3 MHz, within a temperature range of 700-800 °C. Area specific resistance (ASR) values were subsequently determined from the impedance spectra.

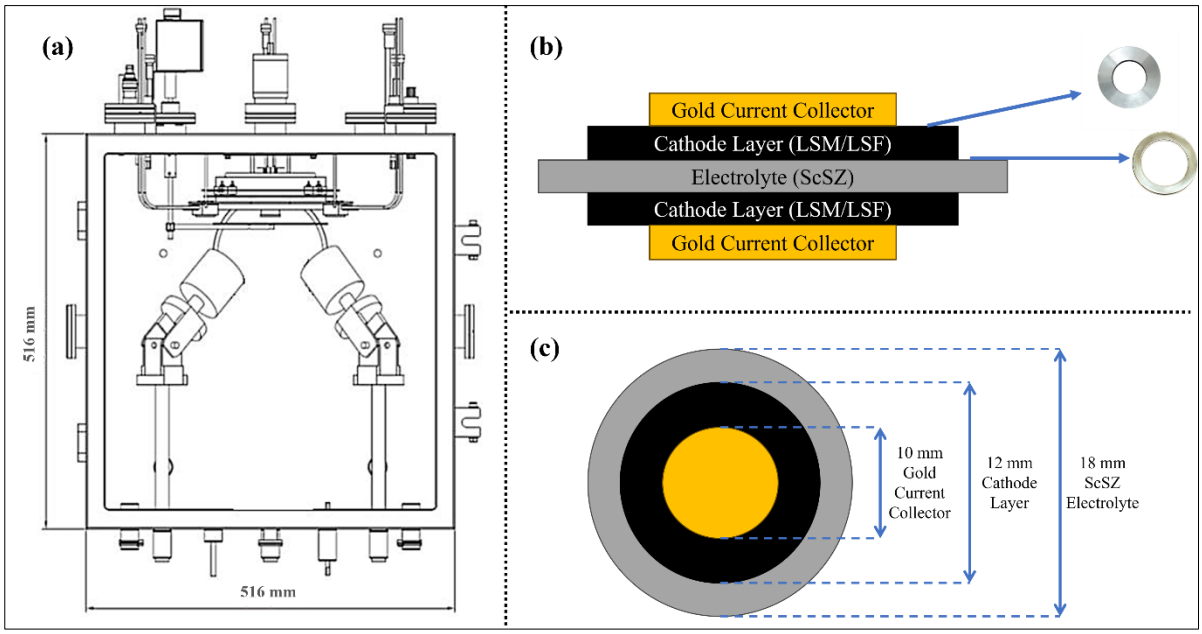

Figure 1 (a) Schematic view of the sputter deposition chamber. (b) Cross-sectional and (c) top view of the symmetrical cells.

3. Results and Discussion

Figure 2 illustrates the TGA outcomes spanning the temperature range from room temperature to 800 °C. This profile unveils a notable decrease in mass commencing at 50 °C, with a subsequent acceleration observed after reaching 200 °C. The mass loss within this temperature range primarily arises from the volatilization of solvent materials, specifically MEK and ethanol, as evidenced by two distinct precipitous declines in the mass-temperature plot. This behavior aligns with earlier investigations, corroborating the solvent evaporation phenomenon [45, 46]. The mass loss tends to diminish beyond 250 °C, approaching near completion by the time the temperature reaches 475 °C. Notably, the mass reduction within the 250-475 °C range can be attributed to the evaporation of the binder material, PVB, and the plasticizer, PEG, in accordance with findings presented by Ceylan et al. [47]. In accordance with the insights gleaned from the TGA results, all ScSZ substrate discs underwent a controlled heating process, ascending at a rate of 0.5 °C per minute up to 700 °C, with a one-hour dwell period at 250 °C. Subsequently, the heating trajectory continued to ascend, reaching 1350 °C at a rate of 1.5 °C per minute, where the discs were sintering for a duration of 2.5 hours.

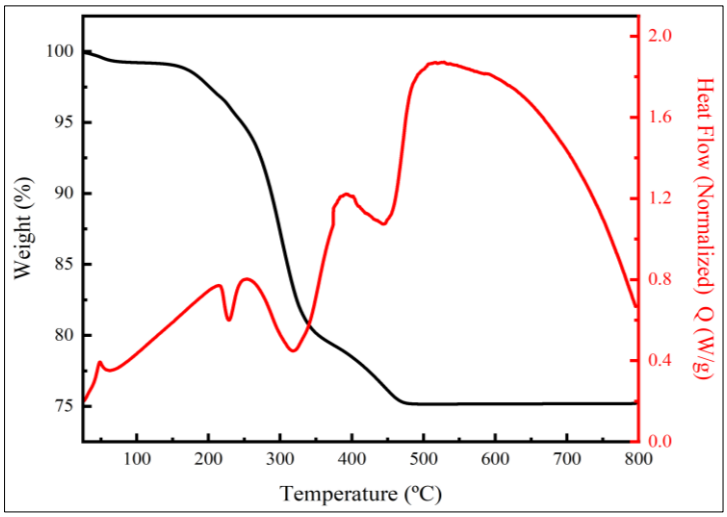

Figure 2 Thermogravimetric analysis of the ScSZ substrate discs from RT to 800 °C.

In Figure 3, we present SEM images depicting the LSM-LSF composite thin film deposited on the ScSZ substrate, along with the EDS analysis results for this film. As seen in Figure 3a, the SEM micrograph illustrates the even distribution of LSM and LSF particles across the substrate's surface. While a top-view inspection might suggest the presence of porosity within the thin film, a cross-sectional view (Figure 3b) unequivocally verifies the formation of a dense and homogeneous composite film atop the substrate, devoid of any discernible porosity or structural defects. Co-sputtered cathode thin films were ordered from 1, the nearest sample to the LSF target, to 6, the nearest sample to the LSM target. To discern the elemental composition of the co-sputtered cathode thin films spanning from 1, representing the nearest proximity to the LSF target, to 6, the closest point to the LSM target, EDS analysis was conducted. Multiple spectra were acquired from each composite thin film's surface, and their average values were subsequently calculated. The resulting data, encompassing the composition of all specimens and the mole fraction of LSM and LSF within the composite thin films, are meticulously documented in Table 1. These findings substantiate the uniformity and structural integrity of the deposited LSM-LSF composite thin film on the ScSZ substrate, further providing essential insights into its elemental composition and compositional balance across the sample set.

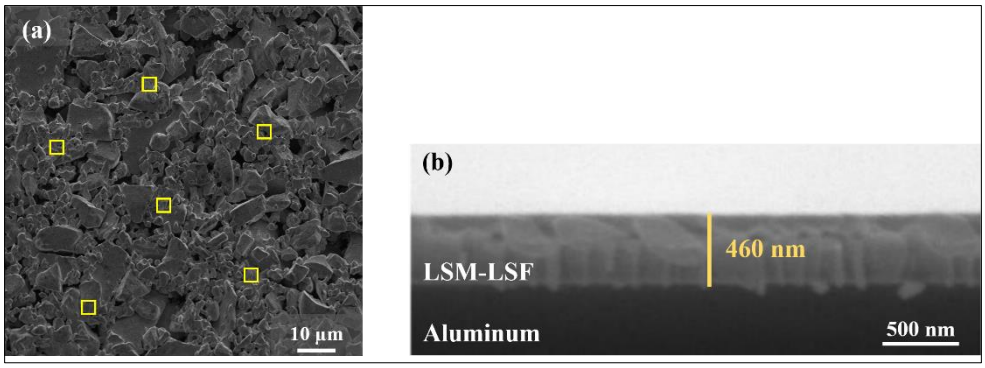

Figure 3 (a) Top view and (b) cross-sectional scanning electron microscopy image of the LSM-LSF composite thin film deposited on ScSZ substrates, respectively.

EIS measurements were systematically carried out for all symmetrical composite LSM-LSF thin films deposited onto ScSZ substrates, encompassing the temperature range from 600 to 800 °C in an air atmosphere. The resulting data, presented in Figure 4a, elucidate the variations in ASR for different composite thin films, as extrapolated from the impedance spectra. Notably, as the temperature escalates, a pronounced reduction in ASR is observed, amounting to an impressive decrease of over three orders of magnitude. This temperature-dependent trend is clearly evident across all composite thin films, underscoring the profound impact of temperature on their electrochemical behavior. For instance, in the case of the composite containing 97% LSF, the ASR plummets from 36.8 $\Omega.cm^2$ at 600 °C to a remarkably low 0.3 $\Omega.cm^2$ at 800 °C. Similarly, for the composite featuring 60 mole percent LSM, the ASR undergoes a comparable reduction, declining from 50 $\Omega.cm^2$ at 600 °C to 0.3 $\Omega.cm^2$ at 800 °C within the same temperature range. Figure 4a also unveils a noteworthy trend pertaining to the effect of LSM mole fraction in the composite thin film on the ASR values. While an

increase in the LSM content generally leads to lower ASR, an optimal composition emerges. Specifically, in the case of the composite thin film comprising 42 mole percent LSM and 58 mole percent LSF, an ASR value of 0.12 Ω.cm^2 at 800 °C is achieved, signifying superior cathode performance compared to counterparts with varying LSM:LSF ratios. Furthermore, considering specific ASR thresholds of 0.15, 0.3, and 1 Ω.cm^2, Figure 4b highlights the distinctive advantages of the LSM42LSF58 cathode. This composite exhibits the lowest working temperature, attaining a remarkable 780 °C, thereby indicating superior ORR activity at lower temperatures compared to alternative cathode configurations (25-28). Importantly, the 0.15 Ω.cm^2 benchmark, denoting effective cathodes, is readily surpassed by the LSM42LSF58 composition, further affirming its outstanding electrochemical performance within the context of solid oxide fuel cell applications.

Table 1 The elemental composition of samples with mole fraction of LSM and LSF in the composite thin films.

Sample No.	Atomic Percent				Mn/Fe Ratio	LSM Mole Fraction	LSF Mole Fraction
	La	Sr	Fe	Mn			
1	31.59	3.13	60.69	4.58	0.07	0.07	0.93
2	32.48	6.29	51.78	9.43	0.18	0.15	0.85
3	29.04	12.17	42.38	16.4	0.38	0.28	0.72
4	28.48	13.92	33.47	24.12	0.72	0.42	0.58
5	27.79	14.98	25.75	31.46	1.22	0.55	0.45
6	29.62	8.89	23.53	37.94	1.61	0.62	0.38

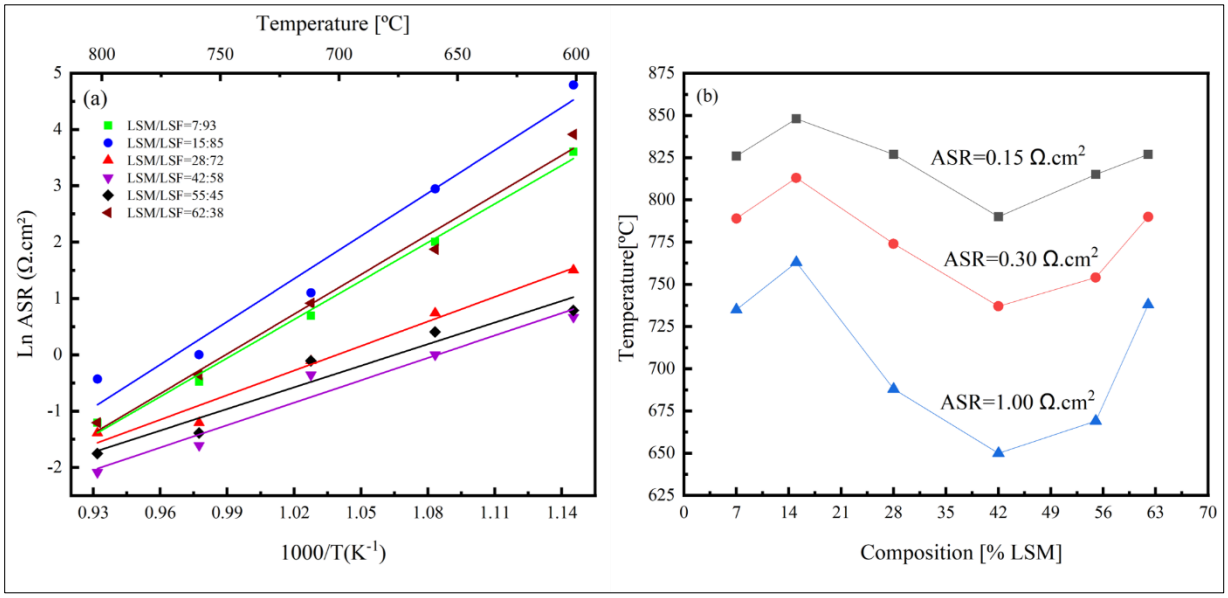

Figure 4 ASR changes versus (a) temperature and (b) molar fraction of LSM in the LSM-LSF composite thin films sputtered on ScSZ.

4. Conclusion

In conclusion, this study offers a comprehensive exploration of the production and characterization of ScSZ electrolyte substrates and composite thin film cathodes composed of LSM and LSF, with a particular focus on their potential utility in SOFCs. To determine optimal sintering conditions, TGA was systematically employed. Furthermore, SEM and EDS were utilized for in-depth examination of microstructural attributes and elemental compositions of the composite films, respectively. Electrochemical performance assessment, conducted via EIS over a temperature range spanning 600 to 800 °C, revealed the mole fraction of LSM within the composite film emerged as a critical determinant of ASR, with an optimal composition consisting of 42 mole percent LSM and 58 mole percent LSF showcasing superior performance.

Most significantly, this composition exhibited an impressively low operational temperature of 780 °C, highlighting its potential as a highly efficient cathode material for SOFC applications.

These findings not only provide valuable insights into the advancement of materials designed for Solid Oxide Fuel Cells but also pave the way for the development of enhanced energy conversion technologies, thus contributing to the broader goals of sustainable energy utilization.

Compliance with ethical standards

Acknowledgments

The author would like to thank the Center for Energy Storage Materials and Devices at the Middle East Technical University. This study did not receive funding from any government or private agency.

Disclosure of Conflict of interest

The author has no conflict of interest in this study.

References

[1] Rajabi R, Sun S, Billings A, Mattick VF, Khan J, Huang K. Insights into Chemical and Electrochemical Interactions between Zn Anode and Electrolytes in Aqueous Zn–ion Batteries. Journal of The Electrochemical Society. 2022;169(11):110536.

[2] Rajabi R, Sun S, Huang K, editors. Performance Comparison of Three Polymer Electrolytes for Zinc Ion Batteries. 243rd ECS Meeting with the 18th International Symposium on Solid Oxide Fuel Cells (SOFC-XVIII); 2023: ECS.

[3] Salmasi F, Sabahi N, Abraham J. Discharge coefficients for rectangular broad-crested gabion weirs: experimental study. Journal of Irrigation and Drainage Engineering. 2021;147(3):04021001.

[4] Taghavi H, El Shafei A, Nasiri A, editors. Liquid Cooling System for a High Power, Medium Frequency, and Medium Voltage Isolated Power Converter. 2023 12th International Conference on Renewable Energy Research and Applications (ICRERA); 2023: IEEE.

[5] Bhuvela P, Taghavi H, Nasiri A, editors. Design Methodology for a Medium Voltage Single Stage LLC Resonant Solar PV Inverter. 2023 12th International Conference on Renewable Energy Research and Applications (ICRERA); 2023: IEEE.

[6] Taghavi M, Perera LP, editors. Data Driven Digital Twin Applications Towards Green Ship Operations. International Conference on Offshore Mechanics and Arctic Engineering; 2022: American Society of Mechanical Engineers.

[7] Taghavi M, Gharehghani A, Nejad FB, Mirsalim M. Developing a model to predict the start of combustion in HCCI engine using ANN-GA approach. Energy Conversion and Management. 2019;195:57-69.

[8] Taghavi M, Perera LP, editors. Multiple Model Adaptive Estimation Coupled With Nonlinear Function Approximation and Gaussian Mixture Models for Predicting Fuel Consumption in Marine Engines. International Conference on Offshore Mechanics and Arctic Engineering; 2023: American Society of Mechanical Engineers.

[9] Taghavi H. Liquid Cooling System for a High Power, Medium Frequency, and Medium Voltage Isolated Power Converter [M.S.]. United States -- South Carolina: University of South Carolina; 2023.

[10] Fan L, Zhu B, Su P-C, He C. Nanomaterials and technologies for low temperature solid oxide fuel cells: recent advances, challenges and opportunities. Nano Energy. 2018;45:148-76.

[11] Soltanizade A, Babaei A, Ataie A, Seyed-Vakili SV. Temperature dependency of activity of nano-catalysts on La 0.6 Sr 0.4 Co 0.2 Fe 0.8 O 3− δ cathode of solid oxide fuel cells. Journal of Applied Electrochemistry. 2019;49:1113-22.

[12] Rajabi R, Raghu S, James R, Huang K, Khan JA, editors. PERFORMANCE COMPARISON OF BATTERY THERMAL MANAGEMENT SYSTEMS BASED ON NUMERICAL SIMULATION. ASTFE Digital Library; 2023: Begel House Inc.

[13] Jeena M, Bok T, Kim SH, Park S, Kim J-Y, Park S, et al. A siloxane-incorporated copolymer as an in situ cross-linkable binder for high performance silicon anodes in Li-ion batteries. Nanoscale. 2016;8(17):9245-53.

[14] Zainon AN, Somalu MR, Bahrain AMK, Muchtar A, Baharuddin NA, SA MA, et al. Challenges in using perovskite-based anode materials for solid oxide fuel cells with various fuels: a review. International Journal of Hydrogen Energy. 2023.

[15] Rostaghi Chalaki H, Babaei A, Ataie A, Seyed-Vakili SV. LaFe 0.6 Co 0.4 O 3 promoted LSCM/YSZ anode for direct utilization of methanol in solid oxide fuel cells. Ionics. 2020;26:1011-8.

[16] Nie Y, Li L, Wei Z. Recent advancements in Pt and Pt-free catalysts for oxygen reduction reaction. Chemical Society Reviews. 2015;44(8):2168-201.

[17] Sreedhar I, Agarwal B, Goyal P, Singh SA. Recent advances in material and performance aspects of solid oxide fuel cells. Journal of Electroanalytical Chemistry. 2019;848:113315.

[18] Kumar RV, Khandale A. A review on recent progress and selection of cobalt-based cathode materials for low temperature-solid oxide fuel cells. Renewable and Sustainable Energy Reviews. 2022;156:111985.

[19] Zhang G, Xiao X, Li B, Gu P, Xue H, Pang H. Transition metal oxides with one-dimensional/one-dimensional-analogue nanostructures for advanced supercapacitors. Journal of Materials Chemistry A. 2017;5(18):8155-86.

[20] Cheng H, Shapter JG, Li Y, Gao G. Recent progress of advanced anode materials of lithium-ion batteries. Journal of Energy Chemistry. 2021;57:451-68.

[21] Chueh WC, Haile SM. Electrochemistry of mixed oxygen ion and electron conducting electrodes in solid electrolyte cells. Annual review of chemical and biomolecular engineering. 2012;3:313-41.

[22] Sun C, Hui R, Roller J. Cathode materials for solid oxide fuel cells: a review. Journal of Solid State Electrochemistry. 2010;14:1125-44.

[23] Chalaki HR, Babaei A, Ataie A, Seyed-Vakili S-V, editors. The Effect of Impregnation of Ceramic Nano-particles on the Performance of LSCM/YSZ Anode Electrode of Solid Oxide Fuel Cell. 5th International Conference on Materials Engineering and Metallurgy; 2016.

[24] Bagi M, Etemadi N, Meekins B, Keshavarz M. Size-Based Microparticle Separation Via Inertial Lift and Dean Flow in a Spiral Microchannel Device. Available at SSRN 4541775.

[25] Burnwal SK, Bharadwaj S, Kistaiah P. Review on MIEC cathode materials for solid oxide fuel cells. Journal of Molecular and Engineering Materials. 2016;4(02):1630001.

[26] Chen K, Lü Z, Chen X, Ai N, Huang X, Du X, et al. Development of LSM-based cathodes for solid oxide fuel cells based on YSZ films. Journal of power sources. 2007;172(2):742-8.

[27] Leonide A, Rüger B, Weber A, Meulenberg W, Ivers-Tiffée E. Impedance study of alternative (La, Sr) FeO3− δ and (La, Sr)(Co, Fe) O3− δ MIEC cathode compositions. Journal of the Electrochemical Society. 2009;157(2):B234.

[28] Leonide A, Rüger B, Weber A, Meulenberg WA, Ivers-Tiffée E. Performance Study of Alternative (La, Sr) FeO3-δ and (La, Sr)(Co, Fe) O3-δ MIEC Cathode Compositions. ECS Transactions. 2009;25(2):2487.

[29] Wang L, Merkle R, Mastrikov YA, Kotomin EA, Maier J. Oxygen exchange kinetics on solid oxide fuel cell cathode materials—general trends and their mechanistic interpretation. Journal of Materials Research. 2012;27(15):2000-8.

[30] Li N, Sun L, Li Q, Xia T, Huo L, Zhao H. Novel and high-performance (La, Sr) MnO3 based composite cathodes for intermediate-temperature solid oxide fuel cells. Journal of the European Ceramic Society. 2023;43(12):5279-87.

[31] Jeong H, Sharma B, Jo S, Kim YH, Myung J-h. Electrochemical characteristics of La0. 8Sr0. 2MnO3 (LSM)–scandia-stabilized zirconia (ScSZ) composite cathode. Journal of the Korean Ceramic Society. 2022;59(4):473-9.

[32] Schmid A, Rupp GM, Fleig J. Voltage and partial pressure dependent defect chemistry in (La, Sr) FeO 3− δ thin films investigated by chemical capacitance measurements. Physical Chemistry Chemical Physics. 2018;20(17):12016-26.

[33] Tang R, Men X, Zhang L, Bi L, Liu Z. Rational modification of traditional La0. 5Sr0. 5 (Fe/Mn) O3 cathodes for proton-conducting solid oxide fuel cells: Inspiration from nature. Ceramics International. 2023.

[34] Dhongde V, Singh A, Kala J, Anjum U, Haider MA, Basu S. Radio-frequency magnetron sputtered thin-film La0. 5Sr0. 5Co0. 95Nb0. 05O3-δ perovskite electrodes for intermediate temperature symmetric solid oxide fuel cell (IT-SSOFC). Materials Reports: Energy. 2022;2(2):100095.

[35] Johnson C, Gemmen R, Orlovskaya N. Nano-structured self-assembled LaCrO3 thin film deposited by RF-magnetron sputtering on a stainless steel interconnect material. Composites Part B: Engineering. 2004;35(2):167-72.

[36] Yang G, El Loubani M, Chalaki HR, Kim J, Keum JK, Rouleau CM, et al. Tuning Ionic Conductivity in Fluorite Gd-Doped CeO2-Bixbyite RE2O3 (RE= Y and Sm) Multilayer Thin Films by Controlling Interfacial Strain. ACS Applied Electronic Materials. 2023.

[37] Xu M, Yu J, Song Y, Ran R, Wang W, Shao Z. Advances in ceramic thin films fabricated by pulsed laser deposition for intermediate-temperature solid oxide fuel cells. Energy & Fuels. 2020;34(9):10568-82.

[38] Chasta G, Himanshu, Dhaka MS. A review on materials, advantages, and challenges in thin film based solid oxide fuel cells. International Journal of Energy Research. 2022;46(11):14627-58.

[39] Tao J, Dong A, Wang J. The influence of microstructure and grain boundary on the electrical properties of scandia stabilized zirconia. Materials Transactions. 2013;54(5):825-32.

[40] Timurkutluk B, Timurkutluk C, Mat MD, Kaplan Y. Development of high-performance anode supported solid oxide fuel cell. International journal of energy research. 2012;36(15):1383-7.

[41] Shen M, Ai F, Ma H, Xu H, Zhang Y. Progress and prospects of reversible solid oxide fuel cell materials. Iscience. 2021;24(12).

[42] Tsipis EV, Kharton VV. Electrode materials and reaction mechanisms in solid oxide fuel cells: A brief review: I Electrochemical behavior vs. materials science aspects. Journal of Solid State Electrochemistry. 2008;12(11):1367-91.

[43] Huang K, Feng M, Goodenough JB, Schmerling M. Characterization of Sr-Doped LaMnO3 and LaCoO3 as cathode materials for a doped LaGaO3 ceramic fuel cell. Journal of the Electrochemical Society. 1996;143(11):3630.

[44] Fossdal A, Menon M, Wærnhus I, Wiik K, Einarsrud MA, Grande T. Crystal structure and thermal expansion of La1− xSrxFeO3− δ materials. Journal of the American Ceramic Society. 2004;87(10):1952-8.

[45] Ren L, Luo X, Zhou H. The tape casting process for manufacturing low-temperature co-fired ceramic green sheets: a review. Journal of the American Ceramic Society. 2018;101(9):3874-89.

[46] Pathak L. Fabrication and sintering characteristics of doctor blade YBCO-Ag tapes. Ceramics international. 2004;30(3):417-27.

[47] Ceylan A, Suvaci E, Mandal H. Role of organic additives on non-aqueous tape casting of SiAlON ceramics. Journal of the European Ceramic Society. 2011;31(1-2):167-73.